or more metal-binding sites in the propeller) detach easily from substrate under shear flow (*35*). The calcium ions in the propeller are not close to the proposed ligand-binding site shown in Fig. 6, but they may help to make more rigid the propeller-thigh interface and may thus regulate integrin-ligand interactions in an allosteric manner. The calcium ion at the thigh–calf-1 interface may play a similar role. Studies with β3 and α5β1 integrins have also shown that a high-affinity Ca^{2+} site is required for ligand-binding, and that a low-affinity Ca^{2+} site allosterically inhibits ligand binding (*36*, *37*). The presence of two adjacent metal-binding sites (MIDAS and ADMIDAS) in the βA domain suggests underlying mechanisms for these effects.

The structure of αVβ3 reveals new domains, previously unpredicted domains, and creative use of the Ig scaffold. Integrin-ligand interactions are regulated not only by changes in affinity but also by altered avidity (receptor clustering) [reviewed in (*38*)]. Integrins also bind in cis to several membrane receptors, an interaction that modulates their signaling functions [reviewed in (*39*)]. The mosaic of domains revealed in the integrin structure can now serve as a foundation for future investigations into the structural basis of these interactions.

References and Notes

1. M. J. Humphries, *Biochem. Soc. Trans.* **28**, 311 (2000).
2. M. A. Arnaout, *Immunol. Rev.* **114**, 145 (1990).
3. R. O. Hynes, *Cell* **69**, 11 (1992).
4. L. V. Parise, D. R. Phillips, *J. Biol. Chem.* **260**, 1750 (1985).
5. M. V. Nermut, N. M. Green, P. Eason, S. S. Yamada, K. M. Yamada, *EMBO J.* **7**, 4093 (1988).
6. J. W. Weisel, C. Nagaswami, G. Vilaire, J. S. Bennett, *J Biol Chem* **267**, 16637 (1992).
7. E.-M. Erb, K. Tangemann, B. Bohrmann, B. Muller, J. Engel, *Biochemistry* **36**, 7395 (1997).
8. K. M. Yamada, B. Geiger, *Curr. Opin. Cell Biol.* **9**, 76 (1997).
9. P. J. Sims, M. H. Ginsberg, E. F. Plow, S. J. Shattil, *J. Biol. Chem.* **266**, 7345 (1991).
10. X. Du *et al.*, *J. Biol. Chem.* **268**, 23087 (1993).
11. R. R. Hantgan, C. Paumi, M. Rocco, J. W. Weisel, *Biochemistry* **38**, 14461 (1999).
12. M. Michishita, V. Videm, M. A. Arnaout, *Cell* **72**, 857 (1993).
13. J.-O. Lee, P. Rieu, M. A. Arnaout, R. Liddington, *Cell* **80**, 631 (1995).
14. B. P. Eliceiri, D. A. Cheresh, *J. Clin. Invest.* **103**, 1227 (1999).
15. E. F. Plow, T. A. Haas, L. Zhang, J. Loftus, J. W. Smith, *J. Biol. Chem.* **275**, 21785 (2000).
16. R. J. Mehta *et al.*, *Biochem J.* **330**, 861 (1998).
17. For additional information, see Web figs. 1 through 7, available at *Science* Online at www.sciencemag.org/cgi/content/full/1064535/DC1.
18. P. Bork, T. Doerks, T. A. Springer, B. Snel, *Trends Biochem. Sci.* **24**, 261 (1999).
19. C. Chothia, E. Y. Jones, *Annu. Rev. Biochem.* **66**, 823 (1997).
20. J.-O. Lee, L. Anne-Bankston, M. A. Arnaout, R. C. Liddington, *Structure* **3**, 1333 (1995).
21. J. Emsley, C. G. Knight, R. W. Farndale, M. J. Barnes, R. C. Liddington, *Cell* **100**, 47 (2000).
22. R. Li, P. Rieu, D. L. Griffith, D. Scott, M. A. Arnaout, *J. Cell Biol.* **143**, 1523 (1998).
23. J. P. Xiong, R. Li, M. Essafi, T. Stehle, M. A. Arnaout, *J. Biol. Chem.* **275**, 38762 (2000).
24. A. K. Downing *et al.*, *Cell* **85**, 597 (1996).
25. L. Holm, C. Sander, *J. Mol. Biol.* **223**, 123 (1993).
26. R. Janowski *et al.*, *Nature Struct. Biol.* **8**, 316 (2001).
27. J. P. Gallivan, D. A. Dougherty, *Proc. Natl. Acad. Sci. U.S.A.* **96**, 9459 (1999).
28. N. Hogg, P. A. Bates, *Matrix Biol.* **19**, 211 (2000).
29. N. Dana, D. F. Fathallah, M. A. Arnaout, *Proc. Natl. Acad. Sci. U.S.A.* **88**, 3106 (1991).
30. P. E. Hughes *et al.*, *J. Biol. Chem.* **271**, 6571 (1996).
31. J. J. Calvete, *Proc. Soc. Exp. Biol. Med.* **222**, 29 (1999).
32. A. P. Mould, A. N. Garratt, W. Puzon-McLaughlin, Y. Takada, M. J. Humphries, *Biochem J.* **331**, 821 (1998).
33. M. A. Wall *et al.*, *Cell* **83**, 1047 (1995).
34. L. A. Fitzgerald, D. R. Phillips, *J. Biol. Chem.* **260**, 11366 (1985).
35. C. Pujades *et al.*, *Mol. Biol. Cell* **8**, 2647 (1997).
36. A. P. Mould, S. K. Akiyama, M. J. Humphries, *J. Biol. Chem.* **270**, 26270 (1995).
37. D. D. Hu, C. F. Barbas, J. W. Smith, *J. Biol. Chem.* **271**, 21745 (1996).
38. Y. van Kooyk, S. J. van Vliet, C. G. Figdor, *J. Biol. Chem.* **274**, 26869 (1999).
39. M. E. Hemler, *Curr. Opin. Cell Biol.* **10**, 578 (1998).
40. M. Carson, *J. Mol. Graph.* **5**, 103 (1987).
41. Single-letter abbreviations for the amino acid residues are as follows: A, Ala; C, Cys; D, Asp; E, Glu; F, Phe; G, Gly; H, His; I, Ile; K, Lys; L, Leu; M, Met; N, Asn; P, Pro; Q, Gln; R, Arg; S, Ser; T, Thr; V, Val; W, Trp; and Y, Tyr.
42. A. Nicholls, K. A. Sharp, B. Honig, *Proteins* **11**, 281 (1991).
43. Z. Otwinowski, W. Minor, *Methods Enzymol.* **276**, 307 (1997).
44. E. de La Fortelle, G. Bricogne, *Methods Enzymol.* **276**, 47 (1997).
45. CCP4, *Acta Crystallogr. D* **50**, 760 (1994).
46. T. A. Jones, J. Y. Zou, S. W. Cowan, M. Kjeldgaard, *Acta Crystallogr. A* **47**, 110 (1991).
47. A. T. Brünger *et al.*, *Acta Crystallogr. D* **54**, 905 (1998).

48. We thank A. Viel, M. Frech, and D. Cheresh for valuable assistance. Supported by NIH grants DK48549, DK50305, HL54227, and AI45716 and a contract from the DOE under contract W-31-109-Eng-38. The coordinates have been deposited in the Protein Data Bank (PDB1JV2).

18 July 2001; accepted 28 August 2001
Published online 6 September 2001;
10.1126/science.1064535
Include this information when citing this paper.

REPORTS

Oxygen Isotopes and the Moon-Forming Giant Impact

U. Wiechert,[1] A. N. Halliday,[1] D.-C. Lee,[1] G. A. Snyder,[2] L. A. Taylor,[2] D. Rumble[3]

We have determined the abundances of ^{16}O, ^{17}O, and ^{18}O in 31 lunar samples from Apollo missions 11, 12, 15, 16, and 17 using a high-precision laser fluorination technique. All oxygen isotope compositions plot within ±0.016 per mil (2 standard deviations) on a single mass-dependent fractionation line that is identical to the terrestrial fractionation line within uncertainties. This observation is consistent with the Giant Impact model, provided that the proto-Earth and the smaller impactor planet (named Theia) formed from an identical mix of components. The similarity between the proto-Earth and Theia is consistent with formation at about the same heliocentric distance. The three oxygen isotopes ($\Delta^{17}O$) provide no evidence that isotopic heterogeneity on the Moon was created by lunar impacts.

The Moon is generally considered to have formed from the debris produced in a collision between the proto-Earth and a Mars-sized impactor (*1*, *2*). Assuming this Giant Impact model to be correct, materials from the proto-Earth, the impactor [named Theia (*3*)], and any additional material added to the Moon after the impact may have introduced isotopic heterogeneity as a consequence of collision and reaccretion. To test for inherent isotopic heterogeneity in the Moon, we searched for small isotopic variations in oxygen. The existing $\Delta^{17}O$ data of three anorthosites, one dunite, one green glass clod, three mineral analyses of a single basalt, and six soil samples from the Apollo missions (*4*) and nine lunar meteorites (*5*) range from −0.204 to +0.094 per mil (‰) (Fig. 1). This large range of 0.3‰ might be because the Moon was not homogeneous, either due to incomplete mixing of material from the proto-Earth and Theia or addition of material to the Moon after the Giant Impact. Here we report the results of new analyses of ^{16}O, ^{17}O and ^{18}O for 31 lunar rocks with the use of a

[1]Institute for Isotope Geology and Mineral Resources, Department of Earth Sciences, ETH Zentrum, Sonneggstrasse 5, 8092 Zürich, Switzerland. [2]Planetary Geosciences Institute, Department of Geological Sciences, University of Tennessee, Knoxville, TN 37996–1410, USA. [3]Geophysical Laboratory, Carnegie Institution of Washington, 5251 Broad Branch Road, Washington, DC 20015, USA.

To whom correspondence should be addressed. E-mail: wiechert@erdw.ethz.ch

higher precision CO_2 laser fluorination technique (*6–10*).

The $\Delta^{17}O$ values of 4 ferroan anorthosites, 15 mare basalts, 2 KREEP basalts, 1 norite, 1 troctolite, 3 lunar volcanic glasses, 4 breccias, and 1 meteorite analyzed for this study yield a range of −0.015 to +0.018‰ (Table 1). Compared with the existing data for lunar meteorites (*5*) and rocks from the Apollo missions (*4*), the range of $\Delta^{17}O$ data is reduced by a factor of 10 (Fig. 1). None of the rock, glass, and breccia samples plot more than 0.018‰ off the terrestrial fractionation line (TFL), which is within the uncertainty of the technique as calculated from 10 analyses of a terrestrial olivine standard $\Delta^{17}O$ = −0.003 ± 0.017‰ (3σ error of the mean). Samples 74220 and 79155 display larger variations in $\Delta^{17}O$ with the use of conventional techniques (*4*) than are obtained with laser fluorination. The differences in $\Delta^{17}O$ among lunar samples obtained by conventional fluorination (*4*, *5*) relate in part to the poorer reproducibility of conventional fluorination. Lunar impacts may also have contributed chondritic material to lunar soils and perhaps created a part of the $\Delta^{17}O$ variation in six lunar soil samples (*4*). However, none of the igneous rocks studied indicates the existence of an isotopically distinct reservoir within the Moon. Nor have $\Delta^{17}O$ variations in glass and breccia samples been identified that were created by lunar impacts.

The reproducibility of laser $\delta^{18}O$ and $\delta^{17}O$ measurements is typically better than ±0.1‰, as documented by duplicate analyses of lunar rocks (Table 1). The $\delta^{18}O$ of picritic, olivine-normative, quartz-normative, and pigeonite mare basalts cannot be distinguished from fresh mid-ocean ridge basalt (MORB) glasses worldwide (*11*), whereas high-Ti mare basalts (TiO_2 > 9%) give $\delta^{18}O$ values lower than MORB glasses. This probably reflects the high normative ilmenite content of the high-Ti mare basalts. There is a systematic difference in $\delta^{18}O$ between lunar basalts and anorthosites that averages 0.4‰ (Table 1). This is most likely caused by equilibrium fractionation between feldspar and silicate melt. In some cases, the apparent $\delta^{18}O$ variation among lunar rocks may reflect sample heterogeneity because the fragments analyzed were small and may therefore have been dominated by disproportionate amounts of olivine, ilmenite, or plagioclase. Only the powdered samples that were used for W isotope measurements should be considered representative of bulk rock samples because of their larger size (>1 g). Despite these reservations, the average $\delta^{18}O$ of the lunar samples is identical to the terrestrial mantle within uncertainty.

The $\Delta^{17}O$ average and reproducibility of all lunar rocks is 0.003 ± 0.005‰ (3σ error of the mean). On the basis of a 99.7 % confidence interval, the lunar and terrestrial fractionation lines are identical to within 0.005‰. Earth and the Moon are distinct, however, from other large planetary bodies like Mars for which the martian meteorite $\Delta^{17}O$ line is displaced by +0.32‰, or asteroid 4 Vesta for which the howardites, eucrites, and diogenites yield $\Delta^{17}O$ values that lie, on average, −0.28‰ below the terrestrial fractionation line (Fig. 2). Besides their differences in $\Delta^{17}O$, Earth and the Moon

Table 1. $\delta^{18}O$ and $\delta^{17}O$ analyses of lunar samples. *n*, number of analyses; p, powdered sample; f, large fragment; 1σ, 1 standard deviation; qtz., quartz; norm., normal; ol., olivine.

Number	Rock type	*n*	Sample type	$\delta^{18}O \pm 1\sigma$	$\delta^{17}O \pm 1\sigma$	$\Delta^{17}O \pm 1\sigma$
			Mare basalts			
12011	Pigeonite basalt	2	p	5.56 ± 0.02	2.92 ± 0.01	0.007 ± 0.023
12045	Ilmenite basalt	2	p	5.34 ± 0.07	2.81 ± 0.05	−0.004 ± 0.010
15058	Qtz-norm. basalt	2	f	5.53 ± 0.07	2.89 ± 0.03	0.013 ± 0.011
15385	Picritic basalt	1	p	5.56	2.93	0.003
15476	Qtz-norm.basalt	2	p	5.58 ± 0.01	2.93 ± 0.03	0.008 ± 0.024
15555	Ol-norm.basalt	2	p	5.36 ± 0.06	2.82 ± 0.03	−0.015 ± 0.001
15556	Ol-norm.basalt	1	f	5.47	2.88 ± 0.05	0.015
15668	Ol-norm.basalt	1	f	5.55	2.92	0.007
10029	High-Ti basalt	1	f	5.43	2.85	−0.003
70035	High-Ti basalt	2	p	5.38 ± 0.02	2.82 ± 0.01	0.005 ± 0.000
71566	High-Ti basalt	2	p	5.31 ± 0.01	2.80 ± 0.00	0.018 ± 0.002
71597	High-Ti basalt	2	p	5.36 ± 0.06	2.83 ± 0.03	0.013 ± 0.006
71539	High-Ti basalt	1	f	5.36	2.81	0.000
75075H	High-Ti basalt	2	p	5.23 ± 0.03	2.76 ± 0.02	0.003 ± 0.003
77516	High-Ti basalt	1	p	5.30	2.79	0.015
			KREEP basalts			
15382		1	p	5.57	2.92	0.006
15386		2	p	5.33 ± 0.04	2.80 ± 0.03	0.000 ± 0.012
			Highland rocks			
15415	Fe-anorthosite	2	p	5.99 ± 0.02	3.14 ± 0.01	−0.008 ± 0.000
60025	Fe-anorthosite	2	p	5.77 ± 0.07	3.02 ± 0.04	0.000 ± 0.008
62255	Fe-anorthosite	2	p	5.94 ± 0.11	3.11 ± 0.06	−0.003 ± 0.001
65315	Fe-anorthosite	2	p	5.59 ± 0.09	2.93 ± 0.06	0.006 ± 0.014
76536T	Troctolite	1	f	5.70	3.00	0.009
77215	Norite	2	p	5.50 ± 0.04	2.89 ± 0.01	0.000 ± 0.006
			Lunar Volcanic glasses			
15426	Green	1	p	5.62	2.94	0.000
74220	Orange	1	p	5.44	2.85	−0.003
74241	Orange	2	f	5.83 ± 0.04	3.06 ± 0.02	−0.012 ± 0.006
			"Breccias"			
10061B	Breccia clast	1	p	5.43	2.84	0.015
10065B	Breccia clast	1	f	5.75	3.03	0.001
60666	Glassy impact melt	1	f	5.51	2.88	0.000
79155	Partialy glass coated gabbro	1	f	6.13	3.22	−0.014
			Meteorite			
ALH 81005		1	f	5.70	2.99	0.000

both yield $\delta^{18}O \sim 5.5‰$ and therefore are, on average, more enriched in ^{18}O than Mars [$\delta^{18}O \sim 4.3‰$ (*12*)] or Vesta [$\delta^{18}O \sim 3.3‰$ (*5*)].

Computer simulations of the Moon-forming Giant Impact indicate that the Moon inherited a significantly higher proportion of material from Theia than the proto-Earth [e.g., see (*1*, *2*)]. The resolution of smooth particle hydrodynamic modeling of potential Moon-forming Giant Impacts has been improved recently. These high-resolution studies show that a potential impactor must have been very close in size to Mars. A significantly larger or smaller impactor would produce a higher angular momentum than observed for the Earth-Moon system or would throw too much iron into orbit, which would have created a more iron-rich Moon (*2*). On the basis of these high-resolution models, it has been estimated that 70 to 90% of the Moon is derived from Theia. An identical oxygen mass fractionation line for the Moon and Earth, therefore, cannot be explained by assuming that similar proportions of material came from the silicate portions of the proto-Earth and Theia. Only if the proto-Earth and Theia $\Delta^{17}O$ values were identical to within 0.03‰ would it be possible that the average $\Delta^{17}O$ value of the Moon plots within 0.005‰ on the terrestrial fractionation line.

Some computer models assume a larger size for the impactor, i.e., a mass ratio of 7:3 between the proto-Earth and Theia (*2*, *13*). All these models assume that the Earth had only achieved about two-thirds of its final mass after the Giant Impact, because a larger proto-Earth would produce greater angular momentum for the Earth-Moon system than that observed. Models assuming that the proto-Earth had reached just 66% of its mass after the Giant Impact (*2*, *3*) and identical $\Delta^{17}O$ of the Moon and Earth require that late incoming material came from the same reservoir as the material that made up Theia and the proto-Earth. If this was another planetesimal, it must have formed from an identical mix of components as the proto-Earth and Theia. Because this is unlikely, the oxygen isotope data are easier to reconcile with a Giant Impact model involving a Mars-sized impactor.

The three isotopes of oxygen are heterogeneously distributed in the solar system (*14*). The largest mass-independent oxygen isotope variations of more than 40‰ are measured on minerals from calcium-aluminum–rich inclusions (CAIs) of the Allende meteorite (*15*, *16*). The different mass-dependent fractionation lines for asteroid 4 Vesta, Mars, and the Earth-Moon system (Fig. 2) provide evidence that the average provenance of the raw material of these objects is significantly different (*5*). There is, however, no obvious relation between oxygen isotopes and current heliocentric distance from the sun as found for $^{53}Cr/^{52}Cr$ (*17*). This might indicate that oxygen isotope compositions were not monotonically zoned through the solar system or that oxygen isotope alteration continued on icy planetesimals (*18*). However, computer simulations of the collisional growth stage of the inner solar system (*19*) demonstrate that terrestrial planets were fed from a zone with a heliocentric distance of 0.5 to 2.5 astronomical units and beyond. Regardless of how heterogeneous the early inner solar system was at the beginning, it developed toward a homogeneous composition by collisional growth. This is endorsed by the small $\Delta^{17}O$ differences of about 0.6‰ observed for the Earth-Moon system, Mars, and Vesta compared with more than 10‰ differences among chondrites. Collisional growth will smooth out pre-existing heterogeneities but is unlikely to result in identical oxygen isotopic compositions for all planets because a correlation between final heliocentric distance and average provenance of a planet is predicted (*19*). The differences in $\Delta^{17}O$ among large planetary embryos and planets depend on final heliocentric distance because oxygen isotopes were heterogeneously distributed in the early solar system. Therefore, the progenitors of the Moon and Earth formed at a similar heliocentric distance. A similar orbit of Theia compared with the proto-Earth would result in a relatively small encounter velocity. This is consistent with the assumptions of most Giant Impact simulations (*20*).

If the proto-Earth and Theia grew from a similar mix of components at a similar distance from the Sun, then not only the oxygen isotopes but also the chemical composition and other isotope ratios should be similar. Therefore, differences between the Moon and Earth, such as the depletion of volatiles or the high FeO content of the lunar mantle compared with the terrestrial mantle, may be of secondary origin. Such differences might be produced during accretion and differentiation of the proto-Earth, Theia, the Moon, and the present Earth (*21*, *22*).

Significant amounts of meteoritic material

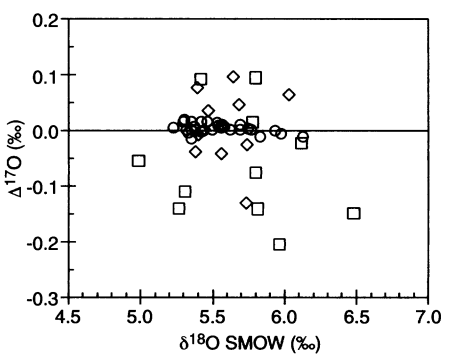

Fig. 1. Comparison between conventional and new laser ^{16}O, ^{17}O, and ^{18}O measurements of lunar samples. $\Delta^{17}O$ gives displacement from the terrestrial fractionation line experimentally defined as $\Delta^{17}O = \delta^{17}O - \delta^{18}O \times 0.5245$. Squares, Apollo Missions (*4*); diamonds, lunar meteorites (*5*); circles, this study.

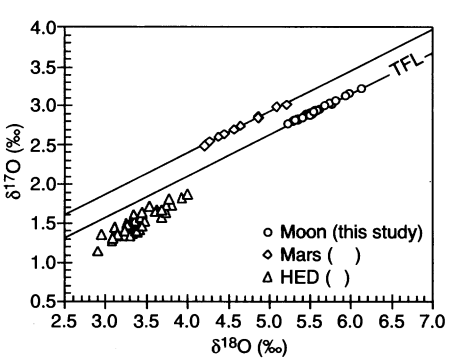

Fig. 2. Three oxygen isotope plots of lunar rocks. Composition of Martian meteorites (*12*) and HED meteorites (*5*), supposed to be fragments of asteroid 4 Vesta, are given for comparison.

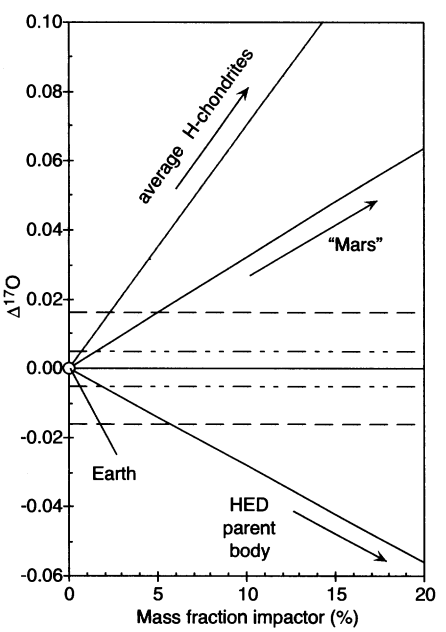

Fig. 3. The $\Delta^{17}O$ values for lunar samples plot within standard deviation ($2\sigma_i$) error of ± 0.016‰ (long-dashed lines) on the TFL. If the impactor had formed from the same raw material as Mars or the HED parent body, then all lunar samples must have obtained, within 2%, the same portion from the impactor and proto-Earth as obtained by Earth using the triple standard error of the mean ($3\sigma_{mean}$) as significant, shown by short-dashed lines. On average, the H-chondrites plot 0.7‰ above the TFL, allowing a maximum of 3% chondritic material mixed into any of the studied lunar samples, 2σ confidence level. Other chondrite groups like L, LL, or carbonaceous chondrites show an even larger deviation from the TFL and, therefore, even less of these primitive materials can be mixed into the lunar samples. For the mixing lines in this figure, identical oxygen abundances have been assumed for all objects.

may have been admixed to the Moon after it formed, perhaps the equivalent of the late veneer on Earth. Although evidence of large impacts is still visible on the surface of the Moon, we have not found any indication of meteoritic material admixed to any of our lunar samples using oxygen isotopes. This does not exclude addition of meteoritic material completely but does limit the amount to several percent. The proportions can be calculated for different meteorite classes. The high (H), low (L), and very low (LL) iron ordinary chondrites are displaced from the TFL by +0.7, +1.0, and +1.3‰ on average (*5*). Admixing 3% H-chondritic material, for example, would be detectable when 0.016‰ deviation is considered significant (Fig. 3). Even less material from L or LL or carbonaceous chondrites would be detectable because these groups are further displaced from the TFL. Although CI-chondrites plot on the TFL, this group is characterized by high $\delta^{18}O$ values above 16‰. Any proportion larger than 5% would increase the $\delta^{18}O$ value by at least 0.5‰. This is also not found for any of the analyzed rocks. Planetesimals with a similar $\Delta^{17}O$ as Mars admixed to any of the lunar samples would need to be present in proportions of >5% to be detectable using oxygen isotopes (Fig. 3). Therefore, we can exclude the possibility that >3 and >5% of these primitive meteoritic or differentiated planetesimals, respectively, have been admixed to any of the studied lunar samples. The only meteorites that are difficult to exclude are the highly reduced enstatite chondrites and aubrites. These have $\Delta^{17}O$ and $\delta^{18}O$ values either identical or very similar to Earth and the Moon (*23*, *24*) and, therefore, could have contributed more than 5% to lunar rocks.

References

1. A. G. W. Cameron, W. Benz, *Icarus* **92**, 204 (1991).
2. A. G. W. Cameron, R. M. Canup, *Lunar Planet Sci* **XXIX**, 1062 (1998); R. M. Canup, E. Asphaug, *Nature* **412**, 708 (2001).
3. A. N. Halliday, *Earth Planet. Sci. Lett.* **176**, 17 (2000a).
4. R. N. Clayton, T. K. Mayeda, *Proc Lunar Sci Conf* **XI**, 1761 (1975).
5. ———, *Geochim. Cosmochim. Acta* **60**, 1999 (1996).
6. Z. D. Sharp, *Geochim. Cosmochim. Acta* **54**, 1353 (1990).
7. D. Rumble III, J. Farquhar, E. D. Young, C. P. Christensen, *Geochim. Cosmochim. Acta* **61**, 4229 (1997).
8. The oxygen isotope ratios of lunar rocks were measured at the Geophysical Laboratory, Carnegie Institution using a Synrad Series 48 CO_2 laser (Synrad, Inc.; Mukilteo, WA) (*6*, *7*). For some samples 1 to 5 small fragments (f) with a total mass between 1.5 and 2.5 mg were reacted in a BrF_5 atmosphere. Powdered samples (p) were melted in vacuum before fluorination in order to avoid losing material by violent reaction of the powder with BrF_5 during laser heating. Surplus BrF_5 and other condensable gases were frozen in liquid nitrogen cold traps. Oxygen was transferred by a Hg-diffusion pump from the metal to the glass line and was frozen on a liquid nitrogen–cooled 5 Å molecular sieve. The function of the diffusion pump is twofold (i) the transport time of oxygen from the sample chamber to the 5 Å molecular sieve is significantly reduced and (ii) tiny amounts of fluorine species (sometimes flushed with the oxygen through the cold traps) are removed by reaction with hot mercury. The isotopic composition was measured on mass 32, 33, and 34 on a MAT-252 dynamic gas source mass spectrometer (Thermo Finnigan MAT; Bremen, Germany). No corrections on mass 33 ($^{17}O^{16}O$) were made because the high-mass resolution of the MAT-252 reduces scattering of $^{32}O_2^-$. The compounds NF_3 and CF_4, which may be produced as by-products during laser fluorination, are known to cause mass interferences at a mass-to-charge ratio (*m/e*) of 33 ($^{17}O^{16}O$) or otherwise interfere with analysis. These compounds were eliminated by preferential adsorption on the 5 Å molecular sieve (*7*). Routine monitoring of these compounds during each analysis by scanning *m/e* 52 (NF_2^+) and 69 (CF_3^+) showed that they were undetectable. The $\delta^{18}O$ value of the reference oxygen has been calibrated to the standard mean ocean water (SMOW) scale with the use of UWG-2, a garnet standard from the University of Wisconsin (*9*). The recommended $\delta^{18}O$ value of UWG-2 is 5.80‰ relative to NIST SRM-28 = 9.60‰. UWG-2 has also been used to define the $\delta^{17}O$ value of the oxygen reference using a value of +3.04‰ on the $\delta^{17}O$ SMOW scale. This value has been calculated from a slope of 0.5245 for the terrestrial fractionation line as defined by 11 minerals with a large range of $\delta^{18}O$ values from 0 to 12‰ and the $\delta^{18}O$ value of UWG-2 using the equation $\delta^{17}O_{(UWG-2)} = \delta^{18}O_{(UWG-2)} * 0.5245$. This equation cannot simply be applied to the oxygen reference gas because the reference gas does lie off the terrestrial fractionation line ($\Delta^{17}O = -0.47$‰).
9. J. Valley, N. Kitchen, M. J. Kohn, C. R. Niendorf, M. Spicuzza, *Geochim. Cosmochim. Acta* **59**, 5223 (1995).
10. We first analyzed terrestrial samples with a wide range of $\delta^{18}O$ from about 0 to 12‰ to be able to detect very small deviations from the mass-dependent terrestrial fractionation line. The linear equation calculated for the terrestrial samples in $\delta^{17}O - \delta^{18}O$ space is $\delta^{17}O = 0.5245 \pm 0.0008 = \delta^{18}$ (2σ confidence level) with a squared correlation coefficient of $R^2 = 0.9999$. Mass-independent displacements are expressed relative to this experimentally determined terrestrial fractionation line as $\Delta^{17}O = \delta^{17}O - 0.5245 * \delta^{18}O$. A terrestrial olivine standard was analyzed together with the lunar samples in every run. Ten analyses of this olivine average $\Delta^{17}O = -0.003 \pm 0.017$ ‰ and 11 analyses of UWG-2 gives 0.001 ± 0.010‰. The overall $\Delta^{17}O$ average of the terrestrial samples is 0.003 ± 0.008‰.
11. J. M. Eiler, P. Schiano, N. Kitchen, E. M. Stolper, *Science* **403**, 530 (2000).
12. I. A. Franchi, I. P. Wright, A. S. Sexton, T. Pillinger, *Meteorit. Planet. Sci.* **34**, 657 (1999).
13. A. G. W. Cameron, *Meteorit. Planet. Sci.* **36**, 9 (2001).
14. R. N. Clayton, *Annu. Rev. Earth Planet. Sci.* **21**, 115 (1993).
15. ———, L. Grossman, T. K. Mayeda, *Science* **182**, 485 (1973).
16. R. N. Clayton, N. Onuma, L. Grossman, T. K. Mayeda, *Earth Planet. Sci. Lett.* **34**, 209-224 (1977).
17. G. W. Lugmair, A. Shukolyukov, *Geochim. Cosmochim. Acta* **62**, 2863 (1998).
18. E. D. Young, R. D. Ash, P. England, D. Rumble III, *Science* **286**, 1331 (1999).
19. G. W. Wetherill, *Geochim. Cosmochim. Acta* **58**, 4513-4520 (1994).
20. W. Benz, personal communication.
21. A. N. Halliday, D. Porcelli, *Earth Planet. Sci. Lett.*, in press.
22. W. Yi *et al.*, *J. Geophys. Res.* **105**, 927 (2000).
23. R. N. Clayton, T. K. Mayeda, *Proc. Lunar Planet. Sci. Conf.* **XV**, C245 (1984).
24. J. Newton, I. A. Franchi, C. T. Pillinger, *Meteorit. Planet. Sci.* **35**, 689 (2000).

25. An early version of this manuscript benefited from reviews of R. Wieler, J. Eiler, and three anonymous reviewers. We acknowledge financial support of the Swiss National Fonds and ETH and the provision of samples by NASA.

1 June 2001; accepted 31 August 2001

Ultrathin Single-Crystalline Silver Nanowire Arrays Formed in an Ambient Solution Phase

Byung Hee Hong, Sung Chul Bae, Chi-Wan Lee, Sukmin Jeong, Kwang S. Kim*

We report the synthesis of single-crystalline silver nanowires of atomic dimensions. The ultrathin silver wires with 0.4 nanometer width grow up to micrometer-scale length inside the pores of self-assembled calix[4]hydroquinone nanotubes by electro-/photochemical redox reaction in an ambient aqueous phase. The present subnanowires are very stable under ambient air and aqueous environments, unlike previously reported metal wires of ~1 nanometer diameter, which existed only transiently in ultrahigh vacuum. The wires exist as coherently oriented three-dimensional arrays of ultrahigh density and thus could be used as model systems for investigating one-dimensional phenomena and as nanoconnectors for designing nanoelectronic devices.

Nanowires have attracted extensive interest in recent years because of their unusual quantum properties and potential use as nanoconnectors and nanoscale devices (*1*–*3*). To possess enhanced physical properties, the wires need to be of small diameter, high aspect ratio, and uniformly oriented (*2*). The stability of the nanowires is also a concern, because metal nanowires of ~1 nm diameter are reported to have existed only transiently (<10 s in ultrahigh vacuum) (*1*, *3*).

We have recently designed, synthesized, and characterized self-assembled organic nanotube arrays (Fig. 1A) formed by calix[4]hydroquinones (CHQs) (Fig. 1B) in the aqueous phase and found that they form chessboard-like arrays of rectangular pores (*4*, *5*). The macrocyclic molecule CHQ is an electrochemically active calixarene derivative with four hydroquinone (HQ) subunits